

Improved Breath Phase and Continuous Adventitious Sound Detection in Lung and Tracheal Sound Using Mixed Set Training and Domain Adaptation

Fu-Shun Hsu^{a,b,c}, Shang-Ran Huang^c, Chang-Fu Su^{a,d,e}, Chien-Wen Huang^f, Yuan-Ren Cheng^{c,g,h},
Chun-Chieh Chen^f, Chun-Yu Wuⁱ, Chung-Wei Chen^b, Yen-Chun Lai^c, Tang-Wei Cheng^c, Nian-Jhen
Lin^{c,j}, Wan-Ling Tsai^c, Ching-Shiang Lu^c, Chuan Chen^c, and Feipei Lai^{a,*}

^a Graduate Institute of Biomedical Electronics and Bioinformatics, National Taiwan University,
Taipei, Taiwan

^b Department of Critical Care Medicine, Far Eastern Memorial Hospital, New Taipei, Taiwan

^c Heroic Faith Medical Science Co., Ltd., Taipei, Taiwan

^d Department of Anesthesia, Division of Medical Quality, En-Chu-Kong Hospital, New Taipei,
Taiwan

^e Department of Electronic Engineering, Oriental Institute of Technology, New Taipei, Taiwan

^f Avalanche Computing Inc., Taipei, Taiwan

^g Department of Life Science, College of Life Science, National Taiwan University, Taipei, Taiwan

^h Institute of Biomedical Sciences, Academia Sinica, Taipei, Taiwan

ⁱ Department of Anesthesiology, National Taiwan University Hospital, Taipei, Taiwan

^j Division of Pulmonary Medicine, Far Eastern Memorial Hospital, New Taipei, Taiwan

***Corresponding Author:** Feipei Lai, Graduate Institute of Biomedical Electronics and Bioinformatics, National Taiwan University, Taipei, Taiwan. (phone: +886-2-3366-4961; Fax: +886-2-3366-3754; e-mail: flai@csie.ntu.edu.tw).

Abstract

Previously, we established a lung sound database, HF_Lung_V2 and proposed convolutional bidirectional gated recurrent unit (CNN-BiGRU) models with adequate ability for inhalation, exhalation, continuous adventitious sound (CAS), and discontinuous adventitious sound detection in the lung sound. In this study, we proceeded to build a tracheal sound database, HF_Tracheal_V1, containing 11107 of 15-second tracheal sound recordings, 23087 inhalation labels, 16728 exhalation labels, and 6874 CAS labels. The tracheal sound in HF_Tracheal_V1 and the lung sound in HF_Lung_V2 were either combined or used alone to train the CNN-BiGRU models for respective lung and tracheal sound analysis. Different training strategies were investigated and compared: (1) using full training (training from scratch) to train the lung sound models using lung sound alone and train the tracheal sound models using tracheal sound alone, (2) using a mixed set that contains both the lung and tracheal sound to train the models, and (3) using domain adaptation that finetuned the pre-trained lung sound models with the tracheal sound data and vice versa. Results showed that the models trained only by lung sound performed poorly in the tracheal sound analysis and vice versa. However, the mixed set training and domain adaptation can improve the performance of exhalation and CAS detection in the lung sound, and inhalation, exhalation, and CAS detection in the tracheal sound compared to positive controls (lung models trained only by lung sound and vice versa). Especially, a model derived from the mixed set training prevails in the situation of killing two birds with one stone.

Keywords: Convolutional neural network, deep learning, domain adaptation, gated-recurrent unit, lung sound, tracheal sound, transfer learning

1. Introduction

Respiratory sound auscultation [1] with a stethoscope is one of the oldest diagnostic techniques used to examine respiratory system of a person. Respiratory sound can be further classified into subtypes, such as mouth sound, tracheal sound, bronchial sound, bronchovesicular and vesicular (lung) sound, depending on where the sound is auscultated [2]. Lung and tracheal sound are the most frequently auscultated in clinical applications.

Lung sound auscultation is commonly used as a first line physical examination tool to diagnose pulmonary disease because it is non-invasive and inexpensive [3]. Breathing with a healthy lung generates normal lung sound, otherwise various types of continuous adventitious sound (CAS), such as wheezes, stridor, and rhonchi, and discontinuous adventitious sound (DAS), such as crackles and pleural friction rubs, are likely to manifest [1, 2]. Healthcare professionals can recognize an abnormal pulmonary condition by knowing the presence, precise type, characteristics and location of the adventitious lung sound [1-3].

Tracheal sound auscultation can be used to detect pulmonary ventilation abnormalities, such as abnormal respiratory rates, upper airway obstruction [4], and apnea. Respiratory rate can be estimated from the identified breath phases in the tracheal sound [5, 6]. The occurrence of partial upper airway obstruction is indicated by the presence of CAS-like patterns, such as stridor [7, 8] and snoring [9], in the tracheal sound. Total upper airway obstruction and apnea can be inferred from the prolonged absence of inhalation and exhalation during tracheal auscultation [6, 8, 10-12].

Therefore, tracheal sound monitoring is recommended by some clinical guidelines to be used in the situation that the pulmonary ventilatory function of a patient is supposed to be frequently compromised, such as during a sedated procedure [13, 14].

Computerized respiratory sound analysis is required in many clinical applications [15, 16]. Previous studies comprehensively reviewed the proposed methods [2, 17]. However, only few research groups [18-20] investigated breath phase and adventitious sound detection in the lung sound at the recording level [2] based on deep learning. Not to mention less effort was made to research tracheal sound analysis using deep learning [21]. In our previous studies, we established lung sound databases, HF_Lung_V1 (Lung_V1) [22] and HF_Lung_V2 (Lung_V2) [23]. Deep learning-based convolutional neural network (CNN)-bidirectional gated recurrent unit (BiGRU) models were proposed and proved to be able to adequately detect inhalation, exhalation, CAS, and DAS events in the lung sound [22, 23]. But we had not yet researched computerized tracheal sound analysis. Thus, we aimed to create a tracheal sound database and train tracheal sound analysis models for breath phase and CAS detection on the basis of deep learning in this study. DAS detection was not included because crackles and pleural friction rubs were not labeled in the collected tracheal sound. Moreover, data size plays an important role in training a more accurate deep learning model [24, 25]; however, collecting and labeling the data are always laborious and expensive. Therefore, it was valuable if we added the collected lung and tracheal sound recordings and labels up to form a bigger dataset for training the deep learning analysis models. However, the lung and tracheal sound have

differences in frequency range, energy drop, the ratio of inhalation to exhalation duration, and pause period [2]. The differences in those acoustic characteristics result in different feature distributions of the lung and tracheal sound. Thus, putting the lung and tracheal sound together for training may produce undesirable results. Should we simply combine the lung and tracheal sound files to form a mixed set to train a single model for both the purposes of the lung and tracheal sound analysis? Or should we use transfer learning [26], specifically domain adaptation [27], to finetune a pre-trained lung sound model for the tracheal sound analysis and vice versa to further improve the model performance? Or should we use full training (training from scratch) [28] strategy to train a lung sound model only on the basis of lung sound and a tracheal sound model only on the basis of tracheal sound? These questions have not been answered in the literature. Hence, the second aim of this study was to investigate what kind of training strategy can make the best lung and tracheal sound models respectively based on the established lung and tracheal sound databases.

2. Materials and Methods

2.1 Establishment of tracheal sound database

The protocol for the tracheal sound study was approved by Joint Institutional Review Board organized by Medical Research Ethical Foundation, Taipei, Taiwan (case number: 19-006-A-2). The

protocol was further reviewed and agreed by En Chu Kong Hospital (case number: ECKIRB1090303). This study was conducted in accordance with the 1964 Helsinki Declaration and its later amendments or comparable ethical standards.

Two hundred and ninety-nine subjects who underwent a surgical procedure with the use of intravenous general anesthesia joined this study. Enrolled subjects were Taiwanese and aged ≥ 20 . The subjects belonged to vulnerable groups (such as prisoners, aboriginals, persons with disabilities, persons with mental illness), those with a history of allergy to contact medical patches or artificial skin, and those mainly diagnosed with atrial fibrillation or arrhythmia were excluded from this study. Tracheal sounds were collected from November, 2019 to June, 2020.

Two devices, HF-Type-2 and 3, were used to record the tracheal sound. HF-Type-2 (Fig. 1a) comprises an electronic stethoscope (AS-101, Heroic Faith Medical Science Co., Ltd., Taipei, Taiwan) connected to a smartphone (Mi 9T pro, Xiaomi, Beijing, China). HF-Type-3 (Fig. 1b) assembly is composed of a chestpiece (603P, Spirit Medical, New Taipei, Taiwan), a stethoscope tubing, a microphone (ECM-PC60, Sony, Minato, Tokyo, Japan), and a smartphone (Mi 9T pro, Xiaomi, Beijing, China). A customized app was installed in the smartphone to record the received tracheal sound. The tracheal sound of each subject was recorded at the flat area in the left or right side of thyroid cartilage as shown in Fig. 2, using one of the devices. Although HF-Type-2 supported multichannel recording, only one channel was used for tracheal sound recording. The tracheal sound was collected at the sampling rate of 4000 Hz with 16 bit depth. The tracheal sound

was recorded when the subjects were undergoing a procedure under intravenous general anesthesia. The recording started before the first administration of anesthetic drug and stopped when the procedure was finished. The recording time varied depending on the need of tracheal sound monitoring, mostly ranging from a few minutes to less than 20 minutes. We did not ask the subjects to take deep breath or hold breath, during the recording. The continuous audio recordings were subsequently truncated to 15-second (s) files with a sliding window with a step size of 15 s; therefore, there was no overlapping between the truncated files. Any tracheal sound file less than 15 s was deleted.

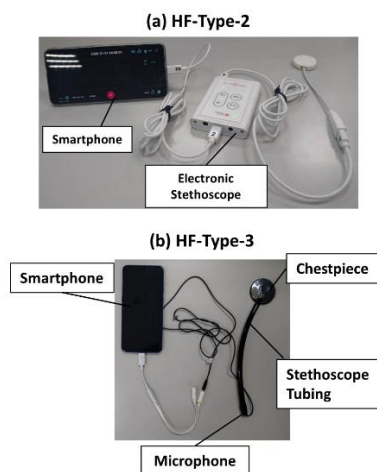


Fig. 1. Photos of HF-Type-2 and 3 devices for tracheal sound recording.



Fig. 2. Recording location of tracheal sound.

Each of the 15-s audio files was subsequently labeled by two labelers, a board-certified respiratory therapist (NJL) with 8 years of clinical experience and a board-certified nurse (WLT) with 13 years of clinical experience. After a file was labeled by one labeler, the quality of the labeling was inspected by another board-certified respiratory therapist (CC) with 6 years of clinical experience or another board-certified nurse (CSL) with 4 years of clinical experience. If the inspector and the labeler did not have an agreement on the labels, the files and labels were further reviewed and corrected if necessary until both had an agreement. After the first labeling of a file, the same labeling and inspection process was repeated by the other group. Intersection was applied on the two obtained sets of labels to create ground-truth labels. The flowchart of ground-truth labels establishment is displayed in Fig. 3. A self-developed labeling software was used to do the labeling [29]. The labelling criteria were maintained by holding regular consensus meetings. Labelers were asked to label the start and end times of inhalation (I), exhalation (E), and CAS (C) events. Unlike the labels in Lung_V1 and Lung_V2, we did not specifically differentiate a CAS into a wheeze, stridor, or rhonchus in tracheal

sounds. It should be noted that CAS labels also included the sound of snoring in this study. Consequently, the tracheal sound files and labels formed HF_Tracheal_V1 (Tracheal_V1) database.

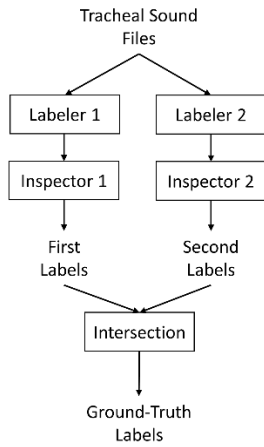


Fig. 3. Flowchart of ground-truth labels establishment.

2.2 Dataset

We divided the tracheal sound recordings and the corresponding labels into training set and test set. The ratio of training to test dataset was intentionally maintained close to 4:1 based on the number of recordings. The truncated files from the same subject can only be assigned to either training or test set. In addition to the Tracheal_V1, the lung sound in Lung_V2 [23] was also used in this study. Hereinafter, the training set and test set of Lung_V2 were denoted by Lung_V2_Train and Lung_V2_Test, respectively. The training set and test set of Tracheal_V1 were denoted by Tracheal_V1_Train and Tracheal_V1_Test, respectively.

2.3 Deep learning pipeline

The CNN-BiGRU model (Fig. 4) outperformed all the other benchmark models in lung sound analysis in our previous study [22]. Therefore, the same CNN-BiGRU model was used in this study.

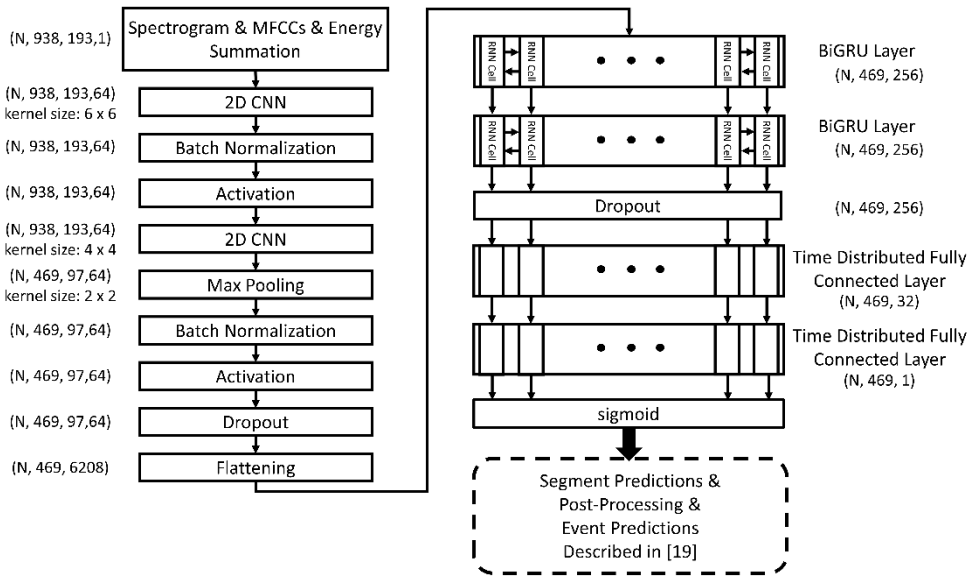


Fig. 4. Architecture of the CNN-BiGRU model.

Two detection tasks, segment detection and event detection, at the recording level were clearly defined in our previous studies [22, 23]. The pipeline of deep learning is presented in Fig. 5, and it was the same as our previous studies [22, 23]. The 15-s signals were first filtered by a Butterworth high-pass filter with a cut-off frequency at 80 Hz. Then, the spectrogram was computed from the 15-s filtered signal using short time Fourier transform [30] with a Hanning window with a size of 256, hop length with a size of 64, and no zero-padding, which rendered a 938×129 matrix, where 938

was the number of time frames (segments) and 129 was the number of the frequency bins. The mel frequency cepstral coefficients (MFCCs) [18] including 20 static coefficients, 20 delta coefficients, and 20 acceleration coefficients were derived from every time segment of the spectrogram so that we had three 938×20 MFCC matrices. The energy in four frequency bands of the spectrogram, namely, 0-250, 250-500, 500-1,000, and 0-2,000 Hz, was summed up to produce four 938×1 energy summation vectors. Normalization was then applied to the spectrogram, each of the three MFCC matrices and each of the energy summation vectors. The concatenation of the normalized spectrogram, MFCCs and energy summation were fed into the CNN-BiGRU model as inputs. The output of the CNN-BiGRU model was a 469×1 probability vector. Thresholding was then applied on the probability vector to get a binarized vector. The value of 1 in an element of the binary vector indicated sound of inhalation, exhalation, or CAS was detected in the corresponding time segment. After the results of segment detection were obtained, the vectors were sent to postprocessing for merging neighboring segments and removing burst events to generate the results of event detection, which is described in the previous studies [22, 23].

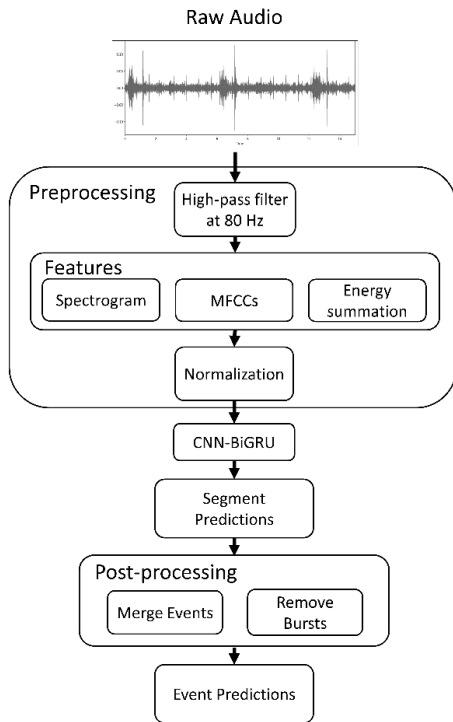


Fig. 5. Deep learning pipeline.

2.4 Training and testing

We tried different training strategies to create different models. First, full training [28] (training from scratch) was used. It meant that lung sound models were trained by Lung_V2_Train alone, and tracheal sound models were trained by Tracheal_V1_Train alone. Second, we mixed the recordings in Lung_V2_Train and Tracheal_V1_Train to form a mixed set to train the models. Third, we used domain adaptation [27] to finetune the pre-trained lung sound models for the tracheal sound analysis, and finetune the pre-trained tracheal sound models for the lung sound analysis. We did not freeze any parameter in the pre-trained model during the domain adaptation. Five-fold cross validation was conducted in each corresponding training dataset for training and validation. All the trained models

were separately tested on both Lung_V2_Test and Tracheal_V1_Test. The models trained by Lung_V2_Train alone and tested by Lung_V2_Test, and trained by Tracheal_V1_Train alone and tested by Tracheal_V1_Test were the positive controls (PCs). The models trained by Lung_V2_Train alone and tested by Tracheal_V1_Test, and the ones trained by Tracheal_V1_Train alone and tested by Lung_V2_Test were the negative controls (NCs). Note that only the recordings contained at least a corresponding label were used to train the model and evaluate the model performance.

The models were trained on a server (OS: Ubuntu 18.04; CPU: Intel(R) Xeon(R) Gold 6154 @3.00 GHz; RAM: 90 GB) provided by the National Center for High-Performance Computing in Taiwan [Taiwan Computing Cloud (TWCC)]. We used TensorFlow 2.10 as the framework to build the deep neural networks. GPU acceleration was run on a NVIDIA Titan V100 card with CUDA 10 and CuDNN 7 frameworks.

2.5 Performance evaluation

The performance of segment and event detection of the models at the recording level was evaluated, respectively, which was the same as the previous studies [22, 23]. We first used the start and end times of the ground-truth event labels in the 15-s recordings (red horizontal bars in Fig. 6a) to create the ground-truth time segments (red vertical bars in Fig. 6b). A segment must have half the duration located within the ground-truth event labels to be designated as a ground-truth time segment. By

comparing the ground-truth time segments (red vertical bars in Fig. 6b) with the results of segment prediction (blue vertical bars in Fig. 6c), we could define true positive (TP; orange vertical bars in Fig. 6d), true negative (TN; green vertical bars in Fig. 6d), false positive (FP; black vertical bars in Fig. 6d), and false negative (FN; yellow vertical bars in Fig. 6d) time segments, which were used to evaluate the performance of segment detection of the models.

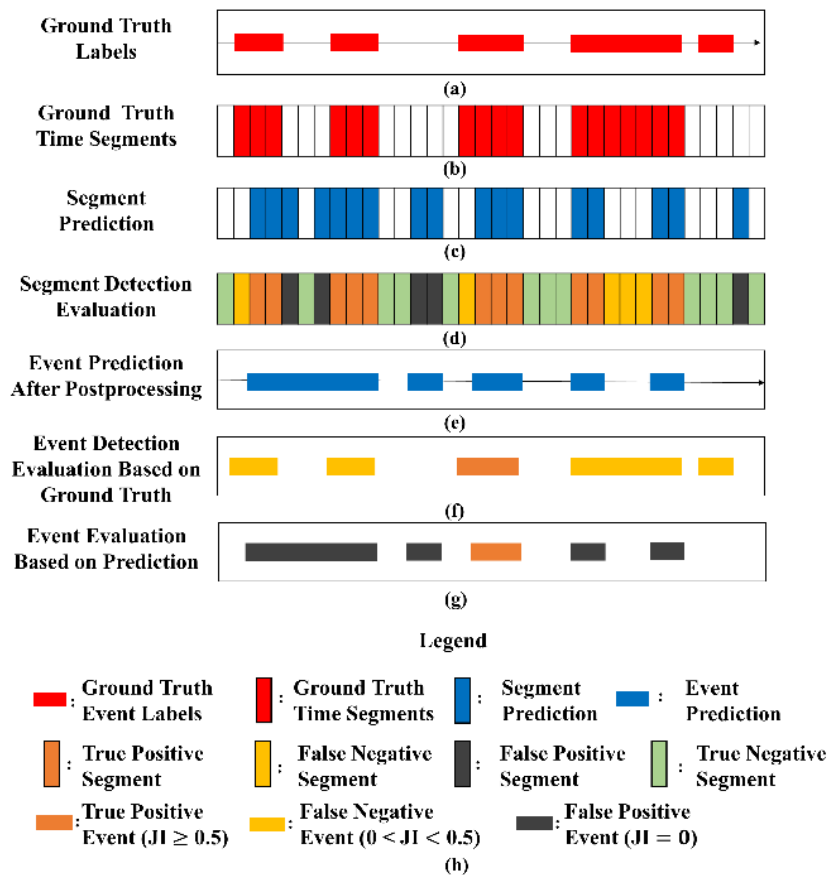


Fig 6. Illustration of segment and event detection evaluation. (a) Ground-truth event labels, (b) ground-truth time segments, (c) segment prediction, (d) segment detection evaluation, (e) event prediction after postprocessing, (f) event detection evaluation based on ground-truth event labels, (g) event evaluation based on event prediction, and (h) legend. JI: Jaccard index.

After we applied the postprocessing to the segment prediction results, we can obtain the results of event prediction (Fig. 6e). Then, Jaccard index (JI) [19] was used to determine whether the models correctly detected an event. Firstly, we used the ground-truth labels as a reference and examined whether every ground-truth label had a predicted event matched to it ($J I \geq 0.5$). If yes, we counted it as a TP event (the orange horizontal bar in Fig 6f); if not, it was an FP event (the yellow horizontal bars in Fig 6f). Then, conversely, we used the event prediction results as a reference; we checked whether we could find a matched ground-truth label for every predicted event ($J I \geq 0.5$). If yes, the predicted event was designated as a TP event (the orange horizontal bar in Fig 6g); if not, it was counted as an FN event (the black horizontal bars in Fig 6g). We did not have a TN event because we did not count the background phase as an event. Note that the TP events were counted twice (the orange horizontal bars in Fig 6f and Fig 6g) as the ground-truth labels and the event prediction results were used as a reference by turns. Therefore, we counted a pair of TP events as a single TP event in the evaluation process (Fig 6f). However, the summed numbers of the FP and FN events were used to compute the evaluation metrics although it may create an undesirable bias in this way.

Similar to our previous studies [22, 23], the performance of segment detection was evaluated with positive predictive value (PPV), accuracy (ACC), sensitivity (SEN), specificity (SPE), F1 score and area under the operating characteristic curve (AUC). However, as we did not have TN events, we only used PPV, SEN and F1 score to evaluate the performance of event detection. The threshold producing the best ACC of segment detection was used to compute PPV, SEN, SPE and F1 score.

We specifically used the F1 score of event detection as the major evaluation metric, because F1 score is a composite measure derived from PPV and SEN and we pursued to accurately detect the start and end times of an event in this study.

3. Results

3.1 Demographic data

Demographic data of the subjects whose tracheal sound was acquired are summarized in Table

1. Total of 299 subjects were enrolled in the study, including 137 males and 162 females. The average age was at 45.7 (95% confidence interval (CI), 18.5–72.9). The average height and weight were 161.5 cm (95% CI, 145.4–177.6 cm) and 63.9 kg (95% CI, 38.6–89.1 kg). The average BMI was 24.3 kg/m² (95% CI, 17.0–31.6 kg/m²). Numbers of patients recorded with HF-Type-2 and 3 were 176 and 123, respectively.

The information of the subjects enrolled to build the Lung_V2 can be found in our previous study [23].

Table 1. Demographic data of the tracheal sound recorded subjects.

Items	Subjects (n=299)
Gender (M/F)	137/162
Age (year)	45.7 (18.5, 72.9)
Height (cm)	161.5 (145.4, 177.6)
Weight (kg)	63.9 (38.6, 89.1)
BMI (kg/m ²)	24.3 (17.0, 31.6)
Recording Devices	
HF-Type-2	176
HF-Type-3	123

The values in the parenthesis represent the 95% confidence interval (CI).

3.2 Summary of Lung_V2 and Tracheal_V1 databases

Summary of Lung_V2 and Tracheal_V1 databases are tabulated in Table 2. There were 14145 15-s recordings, 49659 I labels, 24602 E labels and 22550 C labels in Lung_V2. Tracheal_V1 contains 10958 15-s recordings, 23087 I labels, 16728 E labels and 6874 C labels. The mean duration of I labels was significantly different ($P < 0.001$) between Lung_V2 and Tracheal_V1 (0.95 ± 0.29 s vs 1.09 ± 0.39 s). The mean durations of E labels were significantly different ($P < 0.001$) between Lung_V2 and Tracheal_V1 (0.92 ± 0.49 s vs 0.99 ± 1.07 s). The mean durations of C labels were significantly different between Lung_V2 and Tracheal_V1 (0.82 ± 0.46 s vs 1.07 ± 0.58 s).

Table 2. Summary of HF_Lung_V2 and HF_Tracheal_V1 databases.

Recordings or Labels	Attributes	HF_Lung_V2	HF_Tracheal_V1
Recordings	No.	14145	10958
	Total duration (min)	3536.25	2739.5
I	No.	49659	23087
	Total duration (min)	789.84	420.56
	Mean duration (s)	0.95 ± 0.29	1.09 ± 0.39*
E	No.	24602	16728
	Total duration (min)	376.03	275.36
	Mean duration (s)	0.92 ± 0.49	0.99 ± 1.07*
C	No.	22550	6874
	Total duration (min)	308.21	122.15
	Mean duration (s)	0.82 ± 0.46	1.07 ± 0.58*

I: inhalation labels, E: exhalation labels, and C: continuous adventitious sound labels.

* P-value <0.001 between Lung_V2 and Tracheal_V1.

3.3 Statistics of the training and test datasets

Composition of training and test datasets of both Lung_V2 and Tracheal_V1 databases are summarized in Table 3. There were 10742 and 8700 of 15-second files in Lung_V2_Train and Tracheal_V1_Train, and 3403 and 2258 of 15-second files in Lung_V2_Test and Tracheal_V1_Test. Please refer to Table 3 for the detailed statistics of I, E, and C labels in the training and test datasets of Lung_V2 and Tracheal_V1. The mean duration of I, E and C labels between all the pairs of Lung_V2_Train, Tracheal_V1_Train, Lung_V2_Test and Tracheal_V1_Test is significantly

different (P value <0.001)

Table 3. Training and test datasets of HF_Lung_V2 and HF_Tracheal_V1.

Recordings/ Labels	Attributes	Training datasets		Test datasets		p-value
		Lung_V2	Tracheal_V1	Lung_V2	Tracheal_V1	
Recordings	No.	10742	8700	3403	2258	
	Total duration (min)	2685.5	2175	850.75	564.5	
I	No.	39343	18539	10316	4548	
	Total duration (min)	627.38	343.03	162.46	77.53	
	Mean duration (s)	0.96 ± 0.30	1.11 ± 0.34	0.94 ± 0.26	1.02 ± 0.29	<0.001*
E	No.	18384	13556	6218	3172	
	Total duration (min)	294.67	226.47	81.37	48.89	
	Mean duration (s)	0.96 ± 0.52	1.00 ± 0.41	0.79 ± 0.37	0.92 ± 0.33	<0.001*
C	No.	18353	5955	4197	919	
	Total duration (min)	255.77	106.89	52.45	15.26	
	Mean duration (s)	0.84 ± 0.48	1.08 ± 0.57	0.75 ± 0.34	1.00 ± 0.61	<0.001*

I: inhalation labels, E: exhalation labels, and C: continuous adventitious sound labels.

* indicates the mean duration of I, E and C labels between all the pairs of Lung_V2_Train, Tracheal_V1_Train, Lung_V2_Test and Tracheal_V1_Test is significantly different (P value <0.001), respectively.

3.4 Model Performance

The performance of the trained models for both segment and event detection are tabulated in Table 4. We can observe that all the models trained by mixed set training and domain adaptation had better F1 scores of event detection compared to the NCs (the values with the symbol † in the Table 4). Furthermore, all but one of the models trained by mixed set training and domain adaptation had

F1 scores of event detection greater than or equal to the ones of the PCs (the values with the symbol * in the Table 4).

Table 4. Statistics of model performance.

Controls	Training database /strategy	Test database	Segment Detection						Event Detection		
			ACC	PPV	SEN	SPE	F1	AUC	PPV	SEN	F1
Inhalation											
PC	Lung_V2	Lung_V2	0.933	0.851	0.804	0.965	0.827	0.974	0.901	0.839	0.872
NC	Tracheal_V1	Lung_V2	0.890	0.759	0.658	0.948	0.705	0.934	0.731	0.730	0.750
	Lung_V2+Tracheal_V1	Lung_V2	0.933	0.846	0.809	0.963	0.827	0.974	0.901	0.835	0.872 [†]
	Tracheal_V1→Lung_V2	Lung_V2	0.932	0.847	0.802	0.964	0.824	0.974	0.897	0.831	0.868 [†]
NC	Lung_V2	Tracheal_V1	0.879	0.792	0.573	0.959	0.663	0.902	0.622	0.594	0.669
PC	Tracheal_V1	Tracheal_V1	0.925	0.853	0.771	0.965	0.810	0.964	0.826	0.792	0.831
	Lung_V2+Tracheal_V1	Tracheal_V1	0.927	0.864	0.771	0.968	0.815	0.966	0.830	0.794	0.835 [†]
	Lung_V2→Tracheal_V1	Tracheal_V1	0.930	0.860	0.793	0.966	0.825	0.970	0.844	0.811	0.846 [†]
Exhalation											
PC	Lung_V2	Lung_V2	0.924	0.784	0.641	0.971	0.705	0.953	0.791	0.754	0.806
NC	Tracheal_V1	Lung_V2	0.888	0.664	0.425	0.964	0.518	0.881	0.476	0.489	0.546
	Lung_V2+Tracheal_V1	Lung_V2	0.928	0.785	0.683	0.969	0.730	0.958	0.830	0.788	0.828 [†]
	Tracheal_V1→Lung_V2	Lung_V2	0.926	0.790	0.651	0.971	0.714	0.956	0.802	0.772	0.813 [†]
NC	Lung_V2	Tracheal_V1	0.865	0.729	0.447	0.961	0.554	0.851	0.495	0.512	0.587
PC	Tracheal_V1	Tracheal_V1	0.927	0.846	0.747	0.968	0.793	0.962	0.841	0.797	0.853
	Lung_V2+Tracheal_V1	Tracheal_V1	0.929	0.849	0.755	0.969	0.799	0.963	0.862	0.803	0.861 [†]
	Lung_V2→Tracheal_V1	Tracheal_V1	0.929	0.844	0.763	0.967	0.801	0.963	0.861	0.802	0.859 [†]
Continuous adventitious sound											
PC	Lung_V2	Lung_V2	0.881	0.686	0.442	0.962	0.537	0.913	0.429	0.397	0.491
NC	Tracheal_V1	Lung_V2	0.859	0.588	0.324	0.958	0.417	0.848	0.375	0.310	0.382
	Lung_V2+Tracheal_V1	Lung_V2	0.881	0.667	0.467	0.957	0.549	0.913	0.445	0.407	0.499 [†]
	Tracheal_V1→Lung_V2	Lung_V2	0.883	0.673	0.483	0.957	0.562	0.919	0.482	0.432	0.523 [†]
NC	Lung_V2	Tracheal_V1	0.880	0.726	0.441	0.965	0.545	0.881	0.483	0.437	0.534
PC	Tracheal_V1	Tracheal_V1	0.948	0.848	0.833	0.971	0.840	0.982	0.860	0.775	0.839
	Lung_V2+Tracheal_V1	Tracheal_V1	0.956	0.882	0.841	0.978	0.861	0.986	0.855	0.795	0.871 [†]
	Lung_V2→Tracheal_V1	Tracheal_V1	0.959	0.883	0.863	0.978	0.873	0.987	0.902	0.850	0.898 [†]

PC: positive control, NC: negative control, ACC: accuracy, PPV: positive predictive value, SEN: sensitivity, SPE: specificity, F1: F1 score, and AUC: the area under the receiver operating characteristic curve. Bold values indicate better performance.

Lung_V2+Tracheal_V1 stands for mixed set training. Tracheal_V1→Lung_V2 stands for finetuning the pre-trained tracheal sound model with the lung sound data. Lung_V2→Tracheal_V1 stands for finetuning the pre-trained lung sound model with the tracheal sound data. * indicates the F1 score of event detection of the model is greater than or equal to the one of positive control. † indicates the F1 score of event detection of the model is greater than or equal to the one of negative control.

Table 5 displays the mean F1 scores of event detection derived from averaging the two scores in the Lung_V2_Test and Tracheal_V1_Test. The results clearly show that the models trained by mixed set had the best performance in all tasks if the lung and tracheal sound was not differentiated.

Table 5. Mean F1 scores of inhalation, exhalation, and CAS event detection derived by averaging the two scores in Lung_V2_Test and Tracheal_V1_Test.

Training set/strategy	Label Type		
	I	E	C
Lung_V2	0.770	0.697	0.513
Tracheal_V1	0.791	0.700	0.611
Lung_V2+Tracheal_V1	0.854	0.845	0.685
Tracheal_V1→Lung_V2	0.801	0.762	0.525
Lung_V2→Tracheal_V1	0.822	0.777	0.683

I: inhalation labels, E: exhalation labels, and C: continuous adventitious labels. Bold values indicate the best performance among the four models. Lung_V2+Tracheal_V1 stands for mixed set training. Tracheal_V1→Lung_V2 stands for finetuning the pre-trained tracheal sound model with lung sound data. Lung_V2→Tracheal_V1 stands for finetuning the pre-trained lung sound model with the tracheal sound data.

4. Discussions

Our results show that all the NCs had the worst performance compared to the other models.

Although we did not delve into researching the statistics of feature distribution, the mean duration of I, E and C labels are significantly different between Lung_V2 and Tracheal_V1 (see Table 2), which implies significant differences in the feature distribution between the lung and tracheal sound. Therefore, a model trained by the lung sound has poor performance in the tracheal sound

analysis and vice versa. The majority of the feature distribution differences should be attributed to the innate physical and physiological mechanisms generating the lung and tracheal sound [31].

However, some of the difference may result from that the different recording devices were used to record the lung [22, 23] and tracheal sound.

According to the Table 4, compared to the PCs, all but one of the models trained by mixed set training or domain adaptation had better or equal performance in all the tasks. It implies that the concept of domain adaptation is applicable within the subdomains of respiratory sound. Especially, the Table 5 shows that the model trained by mixed set suffices to do the lung and tracheal sound analysis at the same time. Mixed set training provides an attractive option in developing an all-purpose respiratory monitor that the users do not need to pick specific channels or select specific algorithms for respective lung or tracheal sound analysis.

However, it should be noted that the benefit brought by mixed set training and domain adaptation is not significant in the inhalation detection task on Lung_V2_Test. It may be due to that the number of I labels in the lung sound is relatively large compared to the numbers of the other labels (Table 2 and 3). The domain adaptation is originally proposed to deal with the problem that the data or labels are scarce in the target domain [26, 27]. Therefore, when we have big enough dataset, there is probably no accuracy improvement by using domain adaptation [28].

The model performance of CAS detection in the tracheal sound is considerable better than it in the lung sound (see Table 4). It may result from that the CAS in the tracheal sound is louder, which

makes the signal-to-noise ratio higher so that the CAS patterns are easier to be identified in the tracheal sound. Additionally, the ground-truth labels are checked by four experts in Tracheal_V1, which reduces the number of noisy labels, although the labels in Lung_V2 are not perfect and are currently under a reviewing and correction process [22, 23]. Furthermore, it is speculated that most CAS in Tracheal_V1 is a monophonic event occurred in the inspiratory phase, which characterizes extra-thoracic upper airway obstruction [4] induced by anesthetic drugs, so that the features are not as diverse as the ones in the lung sound in which CAS can be categorized into inspiratory, expiratory and biphasic types, and monophonic and polyphonic events [2].

Unlike what we have done in Lung_V1 and Lung_V2, we do not specifically label DAS in Tracheal_V1. That is because most diseases generating DAS, such as fine crackles, coarse crackles, and pleural friction rubs, do not occur in the upper airway close to pre-tracheal region. However, we occasionally observed DAS-like patterns in our collected tracheal sound. These patterns might be caused by air flowing through accumulation of fluid, such as saliva, sputum, and blood, in the upper airway. Fluid accumulation in the upper airway is a concern that must be tended timely by the healthcare professional in many clinical practices, e.g., having a dental procedure on a moderately or deeply sedated patient who is not able to voluntarily cough out the fluid in the laryngeal region induced by cough reflex [32]. In this case, the dental team needs to do suction to prevent aspiration in the patient. Hence, a respiratory monitor capable of detecting fluid accumulation in the upper airway is of clinical importance. Labeling of DAS-like patterns in tracheal sounds is worth

consideration in the future.

In clinical practice, capnography is more often used to monitor pulmonary ventilation than tracheal sound auscultation. Moreover, an oximeter is a must-have for blood oxygen monitoring during a sedated procedure. However, these devices have some limitations. The accuracy of the capnography is compromised by poor sampling of carbon dioxide caused by open-mouth breathing [33, 34], use of a face mask or nasal cannula [35-37], or a procedure that causes interference of airflow, such as esophagogastroduodenoscopy and bronchoscopy. Not to mention it is hard to use capnography in a surgery involving facial or oral regions. The oxygen desaturation measured by an oximeter is a delayed response to abnormal pulmonary ventilation [38, 39]. Therefore, a tracheal sound monitor that automatically detects abnormal respiratory rate, upper airway obstruction and apnea shows promising clinical values to complement capnography and oximetry [5, 8]. It motivates the development of more accurate tracheal sound analysis models.

5. Conclusion

Automated lung sound and tracheal sound analysis are of clinical values. Lung sound and tracheal sound may have differences in their acoustic features. Therefore, the automated inhalation, exhalation and CAS detection model trained by lung sound alone performs poorly in tracheal sound analysis and vice versa. However, using mixed set training and domain adaptation can improve the

performance of exhalation and CAS detection in the lung sound analysis, and inhalation, exhalation, and CAS detection in the tracheal sound analysis, compared to the PCs (lung models trained only by lung sound and vice versa). Especially, a model derived from the mixed set training can be used in lung sound and tracheal sound analysis simultaneously.

Acknowledgments

The sound collection was sponsored by Raising Children Medical Foundation, Taiwan. The authors thank the employees of Heroic Faith Medical Science Co., Ltd., whoever partially contributed to this study. This manuscript was edited by Wallace Academic Editing. The author would like to acknowledge the National Center for High-Performance Computing (TWCC) in providing computing resources.

References

- [1] A. Bohadana, G. Izbicki, and S. S. Kraman, "Fundamentals of lung auscultation," *New England Journal of Medicine*, vol. 370, no. 8, pp. 744-751, 2014.
- [2] R. X. A. Pramono, S. Bowyer, and E. Rodriguez-Villegas, "Automatic adventitious respiratory sound analysis: A systematic review," *PLoS one*, vol. 12, no. 5, p. e0177926, 2017.
- [3] M. Sarkar, I. Madabhavi, N. Niranjana, and M. Dogra, "Auscultation of the respiratory system," *Annals of thoracic medicine*, vol. 10, no. 3, p. 158, 2015.
- [4] J. C. Acres and M. H. Kryger, "Upper airway obstruction," *Chest*, vol. 80, no. 2, pp. 207-211, 1981.
- [5] K. Ouchi, S. Fujiwara, and K. Sugiyama, "Acoustic method respiratory rate monitoring is useful in patients under intravenous anesthesia," *Journal of clinical monitoring and computing*, vol. 31, no. 1, pp. 59-65, 2017.
- [6] M. A. Ramsay, M. Usman, E. Lagow, M. Mendoza, E. Untalan, and E. De Vol, "The accuracy,

precision and reliability of measuring ventilatory rate and detecting ventilatory pause by rainbow acoustic monitoring and capnometry," *Anesthesia & Analgesia*, vol. 117, no. 1, pp. 69-75, 2013.

- [7] M. Gaffey, "Upper Airway Obstruction," 2020.
- [8] J. P. Boriosi, Q. Zhao, A. Preston, and G. A. Hollman, "The utility of the pretracheal stethoscope in detecting ventilatory abnormalities during propofol sedation in children," *Pediatric Anesthesia*, vol. 29, no. 6, pp. 604-610, 2019.
- [9] A. Yadollahi, E. Giannouli, and Z. Moussavi, "Sleep apnea monitoring and diagnosis based on pulse oximetry and tracheal sound signals," *Medical & biological engineering & computing*, vol. 48, no. 11, pp. 1087-1097, 2010.
- [10] L. Yu *et al.*, "Using the entropy of tracheal sounds to detect apnea during sedation in healthy nonobese volunteers," *Anesthesiology*, vol. 118, no. 6, pp. 1341-1349, 2013.
- [11] J. Liu *et al.*, "Tracheal sounds accurately detect apnea in patients recovering from anesthesia," *Journal of clinical monitoring and computing*, vol. 33, no. 3, pp. 437-444, 2019.
- [12] X. Lu, C. Azevedo Coste, M.-C. Nierat, S. Renaux, T. Similowski, and D. Guiraud, "Respiratory Monitoring Based on Tracheal Sounds: Continuous Time-Frequency Processing of the Phonospirogram Combined with Phonocardiogram-Derived Respiration," *Sensors*, vol. 21, no. 1, p. 99, 2021.
- [13] A. D. Association, "Guidelines for the use of sedation and general anesthesia by dentists," *Adopted by the ADA House of Delegates*, 2016.
- [14] S. S. S. Lives, "WHO guidelines for safe surgery 2009," *Geneva: World Health Organization*, 2009.
- [15] J. Earis and B. Cheetham, "Current methods used for computerized respiratory sound analysis," *European Respiratory Review*, vol. 10, no. 77, pp. 586-590, 2000.
- [16] A. Gurung, C. G. Scrafford, J. M. Tielsch, O. S. Levine, and W. Checkley, "Computerized lung sound analysis as diagnostic aid for the detection of abnormal lung sounds: a systematic review and meta-analysis," *Respiratory medicine*, vol. 105, no. 9, pp. 1396-1403, 2011.
- [17] P. D. Muthusamy, K. Sundaraj, and N. Abd Manap, "Computerized acoustical techniques for respiratory flow-sound analysis: a systematic review," *Artificial Intelligence Review*, vol. 53, no. 5, pp. 3501-3574, 2020.
- [18] E. Messner *et al.*, "Crackle and breathing phase detection in lung sounds with deep bidirectional gated recurrent neural networks," in *2018 40th Annual International Conference of the IEEE Engineering in Medicine and Biology Society (EMBC)*, 2018: IEEE, pp. 356-359.
- [19] C. Jácome, J. Ravn, E. Holsbø, J. C. Aviles-Solis, H. Melbye, and L. Ailo Bongo, "Convolutional neural network for breathing phase detection in lung sounds," *Sensors*, vol. 19, no. 8, p. 1798, 2019.
- [20] C.-H. Hsiao *et al.*, "Breathing Sound Segmentation and Detection Using Transfer Learning

Techniques on an Attention-Based Encoder-Decoder Architecture," in *2020 42nd Annual International Conference of the IEEE Engineering in Medicine & Biology Society (EMBC)*, 2020: IEEE, pp. 754-759.

- [21] H. Nakano, T. Furukawa, and T. Tanigawa, "Tracheal sound analysis using a deep neural network to detect sleep apnea," *Journal of Clinical Sleep Medicine*, vol. 15, no. 8, pp. 1125-1133, 2019.
- [22] F.-S. Hsu *et al.*, "Benchmarking of eight recurrent neural network variants for breath phase and adventitious sound detection on a self-developed open-access lung sound database-HF_Lung_V1," *arXiv preprint arXiv:2102.03049*, 2021.
- [23] F.-S. Hsu *et al.*, "An Update of a Progressively Expanded Database for Automated Lung Sound Analysis," *arXiv preprint arXiv:2102.04062*, 2021.
- [24] J. Hestness *et al.*, "Deep learning scaling is predictable, empirically," *arXiv preprint arXiv:1712.00409*, 2017.
- [25] C. Sun, A. Shrivastava, S. Singh, and A. Gupta, "Revisiting unreasonable effectiveness of data in deep learning era," in *Proceedings of the IEEE international conference on computer vision*, 2017, pp. 843-852.
- [26] K. Weiss, T. M. Khoshgoftaar, and D. Wang, "A survey of transfer learning," *Journal of Big data*, vol. 3, no. 1, pp. 1-40, 2016.
- [27] W. Xu, J. He, and Y. Shu, "Transfer Learning and Deep Domain Adaptation," in *Advances in Deep Learning*: IntechOpen, 2020.
- [28] K. He, R. Girshick, and P. Dollár, "Rethinking imagenet pre-training," in *Proceedings of the IEEE/CVF International Conference on Computer Vision*, 2019, pp. 4918-4927.
- [29] F.-S. Hsu *et al.*, "Development of a Respiratory Sound Labeling Software for Training a Deep Learning-Based Respiratory Sound Analysis Model," *arXiv preprint arXiv:2101.01352*, 2021.
- [30] L. Cohen, *Time-frequency analysis*. Prentice Hall PTR Englewood Cliffs, NJ, 1995.
- [31] N. Goettel and M. J. Herrmann, "Breath Sounds: From Basic Science to Clinical Practice," *Anesthesia & Analgesia*, vol. 128, no. 3, p. e42, 2019.
- [32] H. Hanamoto, M. Sugimura, Y. Morimoto, C. Kudo, A. Boku, and H. Niwa, "Cough reflex under intravenous sedation during dental implant surgery is more frequent during procedures in the maxillary anterior region," *Journal of Oral and Maxillofacial Surgery*, vol. 71, no. 4, pp. e158-e163, 2013.
- [33] R. R. Maddox, C. K. Williams, H. Oglesby, B. Butler, and B. Colclasure, "Clinical experience with patient-controlled analgesia using continuous respiratory monitoring and a smart infusion system," *American journal of health-system pharmacy*, vol. 63, no. 2, pp. 157-164, 2006.
- [34] R. H. Friesen and M. Alswang, "End-tidal PCO₂ monitoring via nasal cannulae in pediatric patients: accuracy and sources of error," *Journal of clinical monitoring*, vol. 12, no. 2, pp. 155-159, 1996.

- [35] J. Hardman, J. Curran, and R. Mahajan, "End-tidal carbon dioxide measurement and breathing system filters," *Anaesthesia*, vol. 52, no. 7, pp. 646-648, 1997.
- [36] M. Patino, D. T. Redford, T. W. Quigley, M. Mahmoud, C. D. Kurth, and P. Szmuk, "Accuracy of acoustic respiration rate monitoring in pediatric patients," *Pediatric Anesthesia*, vol. 23, no. 12, pp. 1166-1173, 2013.
- [37] I. Ahmed, E. Aziz, and N. Newton, "Connection of capnography sampling tube to an intravenous cannula," *Anaesthesia*, vol. 60, no. 8, pp. 824-825, 2005.
- [38] G. Cacho, J. Pérez-Calle, A. Barbado, J. Lledó, R. Ojea, and C. Fernández-Rodríguez, "Capnography is superior to pulse oximetry for the detection of respiratory depression during colonoscopy," *Revista española de enfermedades digestivas*, vol. 102, no. 2, p. 86, 2010.
- [39] T. Lam, M. Nagappa, J. Wong, M. Singh, D. Wong, and F. Chung, "Continuous pulse oximetry and capnography monitoring for postoperative respiratory depression and adverse events: a systematic review and meta-analysis," *Anesthesia & Analgesia*, vol. 125, no. 6, pp. 2019-2029, 2017.